Radiochim. Acta **90**, 623–628 (2002)

The reduction of U(VI) on corroded iron under anoxic conditions

By Daqing Cui[1,*] and Kastriot Spahiu[2]

[1] Studsvik Nuclear AB, S-61182 Nyköping, Sweden
[2] Swedish Nuclear Fuel and Waste Management Co. SE, S-10248, Stockholm, Sweden

(Received August 31, 2001; accepted April 11, 2002)

Uranium / Iron / Green rust / Corrosion product / Reduction

Summary. The corrosion of iron and the interaction between corroded iron and U(VI) in anoxic conditions were investigated. The anoxic conditions were obtained by flushing an 99.97% Ar-0.03% CO_2 gas mixture through the test vessel, in which an oxygen trap and six reaction bottles containing synthetic groundwater (10 mM NaCl and 2 mM HCO_3^-.) were placed. The dark-green coloured corrosion product, formed on iron surface after three months corrosion in synthetic groundwater solutions, was identified by powder X-ray diffraction to be carbonate green rust, $Fe_4^{II}Fe_2^{III}(OH)_{12}CO_3$. The iron foil that reacted in a solution (10 ppm U(VI), 10 mM NaCl and 2 mM HCO_3^-) for three months was analysed by SEM-EDS. The result shows that: (i) an uneven layer of carbonate green rust (1–5 μm thick) formed on the metallic iron; (ii) a thin (0.3 μm) uranium-rich layer deposited on top of the carbonate green rust layer; and (iii) some UO_2 crystals (3–5 μm sized) on the thin uranium layer. The experimental results proved that the U(VI) removal capacity of metal iron is not hindered by formation of a layer of carbonate green rust on the iron. Tests with cast iron and pure iron indicate that they have similar U(VI) removal capacities. At the end of experiment, U concentrations in solution approached the solubility of UO_2 (s), 10^{-8} M. The stability of the carbonate green rust at the experimental conditions, pH, E_h, $[Fe^{2+}]$ and $[HCO_3^-]$, is discussed.

Introduction

Metallic iron is used to remove uranium from contaminated groundwater [1] and as the canister material for nuclear waste disposal [2]. The Swedish spent fuel canister design consists of a copper shell and a massive cast iron insert. The copper shell assures a very long canister life-time (probably millions of years) due to the thermodynamic stability of copper in anoxic groundwaters, while the cast iron insert assures mechanical stability [3]. In performance assessment it is conservatively assumed that some of the canisters are breached and that the spent fuel will get into contact with groundwater in 1000 years [4]. In the case of container failure, the groundwater will contact both the iron of the canister material and the spent nuclear fuel. In this case it is relevant to investigate iron corrosion and its potential role as a chemical barrier for radionuclides eventually released from spent fuel.

*Author for correspondence (E-mail: daqing.cui@studsvik.se).

The reducing effect of iron is expected to dominate over the oxidising effect of gamma-radiolysis in a damaged canister [5]. Thus a reducing environment will prevail in the near field of deep-hard-rock-repository and, therefore, actinide elements and Tc should be in their sparingly soluble tri- and tetravalent oxidation states. Under anoxic conditions, iron reacts with water by producing hydrogen gas and form magnetite, Fe_3O_4, as the corrosion product [6, 7]. Another type of iron corrosion product is Fe(II)-Fe(III) hydroxy compounds containing a certain amount of a non-hydroxyl anion (CO_3^{2-}, Cl^-, or SO_4^-) and having higher specific surface area and higher anion adsorption capacity, also called green rusts (GR). The GR containing carbonate (GR_C) is formed by the oxidation of Fe^0 in $NaHCO_3$ solution with pH 8 at potentials around −0.3 V (*vs*. SHE) [8] or by oxidation of $Fe(OH)_2$ in HCO_3^- solutions [9]. Occurrences of Fe(II)-Fe(III) GR in hydromorphic soils [10] and in inner corrosion films of iron water-pipes [7] have been reported. The composition of GR_C ($Fe_4^{II}Fe_2^{III}(OH)_{12}CO_3$) and its X-ray diffraction patterns were determined [11].

It is expected that formation of GRs should be a common process in anoxic non-acid aqueous systems both in nature and laboratories [7, 12, 13]. However the high reactivity of the GRs including its oxidation by dioxygen during sampling, handling and analysis is probably the main reason that GRs have not often been identified in mineralogical analyses [13]. The examination of GRs by different instrumental techniques is only possible if oxidation is prevented. The reduction of Cr(VI) to Cr(III) by GRs was found to be a very fast reaction [14]. The reduction of chromate by carbonate green rust (GR_C) at pH 7 follows first order kinetics with respect to Cr(VI) at higher surface area concentrations [15].

Uranium is an important element in the context of the overall nuclear fuel circle from mining to waste disposal. UO_2 is the main component of the spent fuel matrix. Together with its daughter nuclides, uranium will contribute significantly to the overall radiological impact of the repository after 10^5 years of disposal [16]. Under oxic carbonate containing groundwaters, U(VI) is soluble. However, under sufficiently low redox potentials, U(VI) may be reduced to UO_2 (s) with a solubility around 10^{-8} M in the pH range between 4 and 14 [17]. The removal of U(VI) from groundwater by using metallic iron [1, 18, 19] and by iron corrosion products formed in saline solution [20] has been reported. The uranium can also be electrochemically removed from solution by iron electrodes. Uranium(IV) was found

to be incorporated into GR that formed during the electrochemical process [21]. No information is given (a) if the U(IV) reduced by iron precipitates as uraninite (UO_2 (s)) or if it is co-precipitated by the iron corrosion product, and (b) the distribution of the reduced U(IV) across the iron-water interface.

The present work focuses on the behaviour of dissolved U(VI) in the presence of corroded iron metal in a simulated anoxic groundwater solution (10 mM NaCl and 2 mM HCO_3^-, pH 8.5) and attempts to address the following questions:

(a) What is the major corrosion product of metallic iron?
(b) Do the formation of iron corrosion products influences U(VI) removal capacity of metallic iron?
(c) In which mineral form is uranium "immobilised" by the corroded iron?
(d) How is "immobilised" uranium distributed across the iron-groundwater interface?

Experimental

Materials and analytical methods

Iron grains of 99.99% purity, iron foils with purity 99.998%, and cast iron 1002, (SS0717-00) were purchased. Iron foils and cast iron were cut and polished with Silicon Carbide paper (#500, #2000, #4000). Acetone was used as coolant during the last polishing step. To avoid oxidation, all iron samples (before and after reaction) were kept in desiccator filled with Ar gas.

Solution A (10 mM NaCl, 2 mM HCO_3^-, pH 8.5) and solution B (30 ppm U(VI), 10 mM NaCl, 2 mM HCO_3^-, pH 8.5) were prepared using analytical grade salts and deionised water. The potential existence of U(VI) particles in solution B was checked by filtration of the solution through a 0.45 μm pore size filter. Within uncertainty limits, the same uranium (VI) concentrations before and after filtration were observed, meaning that there was no significant solid form of U(VI) in the solution. Uranium concentration was analysed by a laser induced fluorescence analyser (UA-3). The iron concentration was determined by ICP-OES (Inductively Coupled Plasma-Optical Emission Spectrometry).

The corrosion products were analysed by a X-ray diffraction (XRD) Guinier camera with Cu $K_{\alpha 1}$ wavelength 1.5406 Å. After pre-calibration, the diffraction patterns (d (Å) and intensity values) were recorded on CEA-15 REFLEX film and read either by LS-20 Scanner or by naked eyes with help of a d (Å) ruler.

SEM (Scanning Electron Microscopy)-EDS (Energy Dispersive Spectra) were used to check the microstructure and elemental composition of the corrosion products and of the immobilised uranium on iron surface.

Experimental arrangement

In the study of iron corrosion and Fe^0-U(VI) redox reaction under anoxic conditions, our experience has shown that the largest difficulty is the control of anoxic conditions. The experiment setup for the present work is shown in Fig. 1. Glass reaction bottles A–F (25 mL) and an oxygen trap vessel

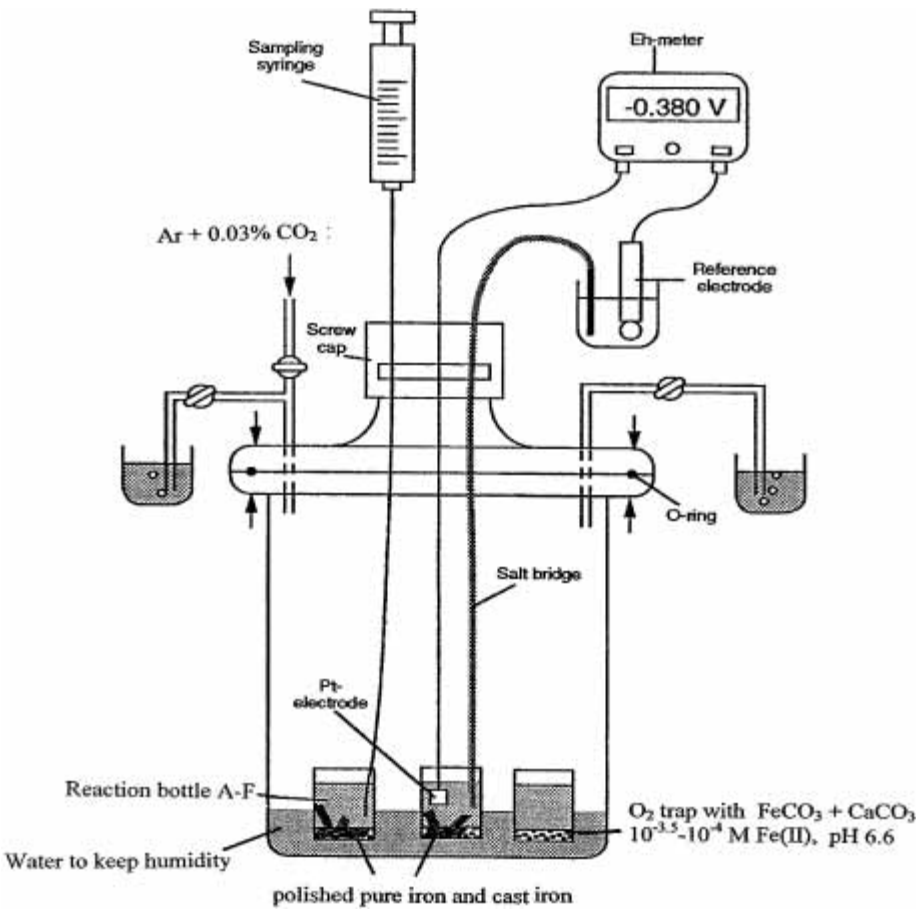

Fig. 1. Experimental arrangement for the investigation of iron corrosion and iron-uranium redox reaction. In the vessel, several batch experiments were carried out in bottles A–F, as described in Table 1.

Table 1. Description of batch experiments in reaction bottles A–F.

Reaction bottles	Iron type	Surface area, cm^2	$C_{U(VI)}$ ppm	Time before adding U, d	Reaction t, d	Analysed items
A	pure iron grain	4	0	not added	90	SEM-EDS, XRD
B	pure iron foil	1.06	10	0	90	SEM-EDS, XRD
C	cast iron coupon	4	1	0.5	44	$C_{U(VI)}$ $C_{Fe(II)}$, pH, E_h
D	cast iron coupon	4	1	38	81	$C_{U(VI)}$ $C_{Fe(II)}$, pH, E_h
E	pure iron foil	1.06	1	0.5	44	$C_{U(VI)}$ $C_{Fe(II)}$, pH, E_h
F	pure iron foil	1.06	1	38	81	$C_{U(VI)}$ $C_{Fe(II)}$, pH, E_h

containing 2 g $FeCO_3$ – 2.5 $CaCO_3$ and 50 mL solution were placed inside a 10 L glass vessel, as shown in Fig. 1. All gas tubes, valves and connections were made of stainless steel and are tight against O_2 diffusion. Both Fe^{2+} concentration and pH in the O_2-trap are buffered by the solids. After six months in the reaction vessel, the solution in the trap had a blue-green colour and the pH of the solution was 6.73 ± 0.02. Traces of O_2 present in the flushing gas or diffused in the vessel were preferentially captured in the oxygen trap vessel. All bottles A–F were exposed at the same atmosphere and hence comparable results of batch reactions were achieved. To minimise the evaporation of solutions in bottles A–F, 300 mL solution A was added on the bottom of the vessel.

The following experimental and chemical analytical steps were performed at a controlled temperature 22.0 ± 2.0 °C:

- Flushing the vessel with a 99.97% Ar-0.03% CO_2 gas mixture (AGA, Plus grade, < 2 ppm impurities) to reach anoxic conditions, repeatedly evacuating and gas purging three times.
- Preparation of solutions containing certain U(VI) concentrations, as described in Table 1, from solutions A and B. Addition of the deoxygenated solutions (20 mL) into bottles A–F by using a syringe.
- After flushing the vessel with the gas mixture for one day, iron grains, polished iron foils and cast iron coupons were added into bottles by using a magnetic bar through the screw-cap opening (Fig. 1 and Table 1). Whenever the screw-cap and rubber membrane were removed, to avoid oxygen contamination, a higher speed flushing of Ar-CO_2 gas mixture was applied.
- After different reaction times (Table 1), solution samples were taken by using a syringe through the rubber membrane screw-cap. The samples were acidified to avoid Fe(III) precipitation and consequent U(VI) sorption on the iron precipitate.
- After three months experiment, corroded iron samples in bottles A and B were removed through the screw cap opening by using a magnetic bar and thereafter quickly dried in vacuum. The corrosion products were scraped off in an inflatable Ar-filled bag and transported in the Ar filled desiccator for XRD identification.
- The iron foil reacted in bottle B for 90 days was embedded in EPOXY polymer. The cross section was polished and analysed with SEM-EDS.
- The effects of formation of corrosion products on uranium removal by cast iron and pure iron were studied through the batch experiments in reaction bottles C to F, as described in Table 1.
- Redox potentials of the solutions in the reaction bottles (C–F) were measured by using a salt bridge (3 M KCl Agar-Agar) connected to a reference electrode (Ag/AgCl, 3 M Cl^-) and a Pt electrode penetrated through the rubber membrane on the screw cap. The pH values were measured by a combined pH electrode inserted through the screw-cap opening.

Result and discussion

Kinetics of Fe-U(VI) redox reaction

The kinetics of U(VI) removal by corroded metallic iron was investigated by measuring the uranium concentration in solution in bottles C–F at different times. The results are shown in Fig. 2. In this work, the reductive sites on the iron surface should be in excess of U(VI), as seen from the nearly linear relationship between $\log C_t/C_0$ and reaction time (except for the initial period), where C_0 and C_t are U(VI) concentrations at time 0 and t respectively. This indicates that the uranium removal closely approximates pseudo-first order reaction kinetics. In Fig. 2, the kinetic data from this work are compared with data (open circles) of

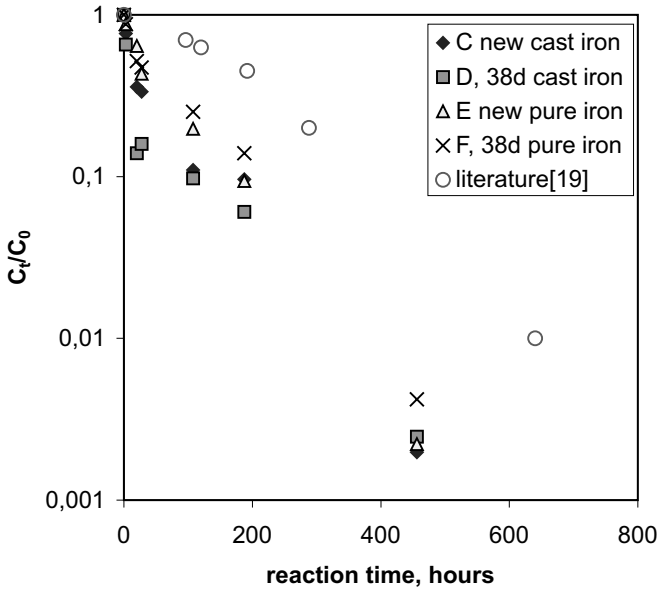

Fig. 2. U(VI) removal by iron coupons as a function of reaction time. 1.06 cm^2 pure iron foils and 4.0 cm^2 cast iron coupon were added for 12 hours or for 38 days in a 20 mL solution initially containing 10 mM NaCl and 2 mM HCO_3^-. The initial U(VI) concentration is 1000 ppb. C–F indicates the batch experiments described in Table 1. The open circles show the data from a previous experiment with 3.9 cm^2 iron coupon and 500 mL solution [19]. C_0 and C_t are U(VI) concentrations at time 0 and t, respectively.

Farrell *et al*. [19]. The slower kinetics of U(VI) removal may be caused by the ~ 4 times lower iron surface/liquid volume ratio and/or using a different anoxic solution (0.4 M NaCl) in that work.

It has been shown that multielectron redox reactions between negatively charged species (*e.g*. TcO_4^-, CrO_4^{2-}) and Fe(II) minerals involve a sorption and surface reductive precipitation mechanism [22]. If the surface sites are in excess, the reaction will follow first order reaction kinetics [14, 15, 23].

As may be observed from Fig. 2, both pure iron and cast iron samples corroded for 38 days display a slightly faster initial U(VI) removal than the newly added iron samples. This may be due to the process that iron corrosion products absorb $UO_2(CO_3)_3^{4-}$ (the predominant species of U(VI) at the experimental condition) enhancing thus the initial U(VI) removal process. This hypothesis is supported by the microscopic analysis of outer surfaces that will be discussed below.

The differences in U(VI) removal by pure iron and cast iron foils are mainly caused by difference in their surface areas (Table 1). It may be concluded that under our experimental conditions, U(VI) removal per unit surface area does not strongly depend on the type of iron (pure iron or cast iron) or the existence of corrosion product. At the end of the experiments, the uranium concentration was approaching the UO_2 (s) solubility level, 10^{-8} M [17].

XRD and microscopic analysis of iron corrosion product and uranium phase

A layer (0.5–1 μm) of corrosion product was observed in SEM micrographs of a cross section of a pure iron grain that reacted in bottle A for 90 days. The X-ray diffraction pattern of the scraped dark-green coloured corrosion product is given in Table 2. The reported data of an iron carbonate hydroxide, also called carbonate green rust (GR_C), $Fe_4^{II}Fe_2^{III}(OH)_{12}CO_3$, (JCPDS number 46-0098) [12], are given for comparison. The *d* (Å) and intensity values of the diffraction peaks of the corrosion product are in a good agreement with the reported values for $Fe_4^{II}Fe_2^{III}(OH)_{12}CO_3$.

After three months reaction in bottle B, the iron foil was still light-reflecting, except for ~ 30% of its surface being covered by dark-green coloured specks. The result of XRD analysis of the scraped sample of these specks demonstrates the existences of two minerals: GR_C, that is the same as these found on pure iron grains, and uraninite UO_2 (s).

Except GR_C, no other iron minerals were detected in the corrosion products formed in bottles A and B. It means that, in our experiment conditions, GR_C is a stable corrosion product, but not $Fe(OH)_2$, Fe_3O_4 and $Fe(OH)_3$. Possible explanations are (a) metallic iron and ppm levels of Fe(II) in solution have enough redox buffer capacity to prevent GR_C from oxidation to Fe_3O_4 and $Fe(OH)_3$ or/and (b) GR_C may have semi-conductive properties, in the meaning that electrons may be transferred from Fe^0 to the outer surface of GR_C. The pH-E_h-[Fe^{2+}] diagram of the iron system with the stability field of GR_C was reproduced based on data from [10], as shown in Fig. 3. The stability of GR_C at our experimental conditions (pH, E_h and [Fe^{2+}]) will be further discussed below.

SEM micrographs of a cross section of the iron foil reacted in bottle B are shown in Fig. 4a. EDS analysis for the selected points A–E in Fig. 4a are given in Table 3. The data given in Table 3 are the semi-quantitative raw data from EDS measurement without calibration and mathematical treatment. The marked points in Fig. 4a, (A) and (B) are the thin uranium layer deposited on GR_C layer; (C) and (D) are green rust, and (E) is a uraninite crystal; The EDS element profile

Table 2. The data of XRD for the corrosion product and reported data for green rust $Fe_4^{II}Fe_2^{III}(OH)_{12}CO_3$.

Measured		Reported [11]				
d (Å)	Intensity	*d* (Å)	Intensity	*h*	*k*	*l*
7.549[a]	100	7.530	100	0	0	3
3.748[a]	28	3.759	32	0	0	6
2.733[b]	1	2.720	1	1	0	1
2.662[a]	26.5	2.668	15	0	1	2
2.47[b]	3	2.470	3	1	0	4
2.340[a]	15	2.344	12	0	1	5
2.09[b]	1	2.09	1	1	0	7
1.96[b]	7	1.967	9	0	1	8
[c]	–	1.880	1	0	0	12
1.74[b]	1	1.740	2	1	0	10
1.64[b]	1	1.644	1	0	1	11
1.58[b]	2	1.583	2	1	1	0
1.54[b]	1	1.55	2	1	1	3
1.46[b]	1	1.462	2	1	1	6

a: strong diffraction lines read by scanner;
b: weak diffraction lines read by naked eyes;
c: not found.

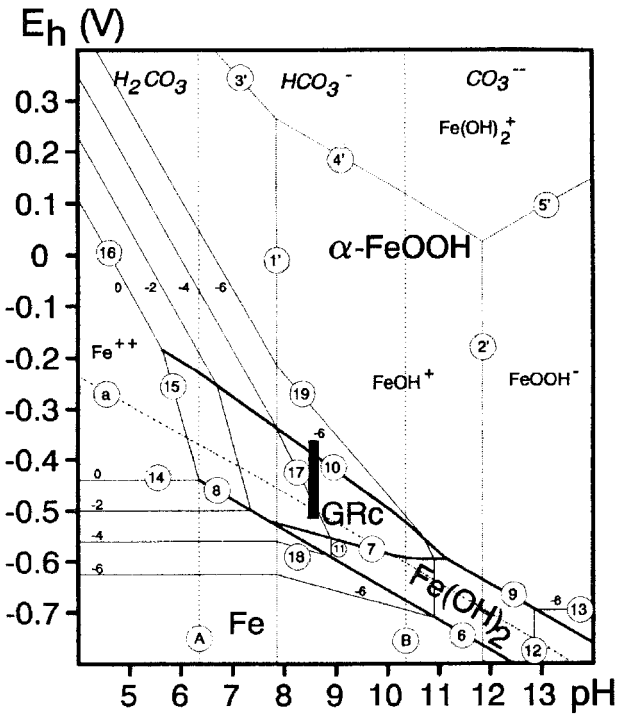

Fig. 3. Pourbaix pH-E_h diagram for the carbonate green rust, regenerated based on [10]. pH-E_h values for the solutions in react bottles C, D, E and F (see Table 2) are all within the triangle for GRc (carbonate green rust) as marked by the solid bar. $-n$ means $[Fe^{2+}] = 10^{-n}$. The equilibrium equations represented by the lines with circled numbers are listed in [10].

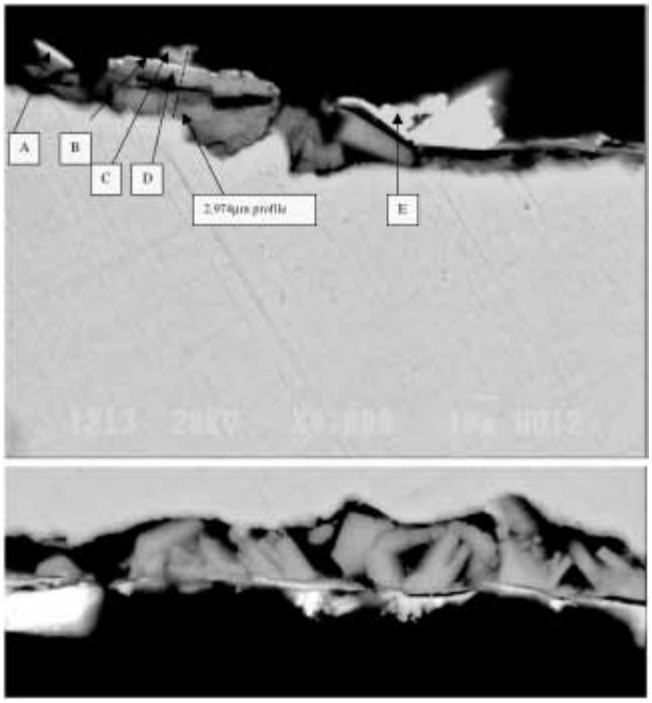

ⓐ

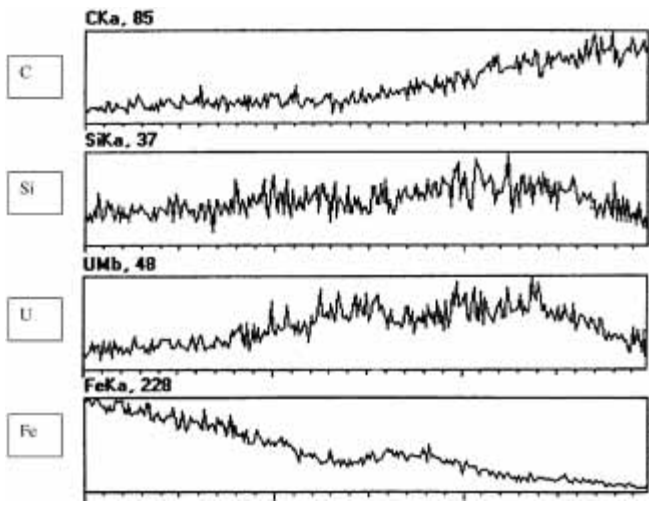

ⓑ

Fig. 4. (**a**) SEM micrograph of the cross section of the outer-surface of an iron coupon reacted for 3 months in a solution initially containing 10 ppm U(VI), 10 mM NaCl and 2 mM HCO_3^-. The white, black, light grey and dark grey parts represent uraninite crystals, EPROXY polymer, iron metal and GRc, respectively. (**b**) Element profiles across the outer surface along the dotted line marked in (**a**). Results of EDS analysis for the arrowed points A–E are listed in Table 3.

across the outer surface, marked as a dotted line in Fig. 4a, is shown in Fig. 4b.

The following observations can be summarised:

i. An uneven layer of GR_C (1–5 μm) forms on iron surface.
ii. GR_C is in the form of 1–5 μm sized crystals.
iii. A thin (0.3 μm) uranium-rich layer is deposited on top of GR_C. Some UO_2 (s) crystals, 3–5 μm sized, shown by (E) in Fig. 4a, were formed on the top of the thin uranium-rich layer, in agreement with the results of XRD analysis and the very low uranium concentration (near UO_2 solubility) in bottles C–F at the end of the experiments. The EDS mapping of the cross section shows that uranium is not found to be incorporated into GR_C crystals, instead forms UO_2 (s) crystals on GR_C. This is in disagreement with a previous observation [21].
iv. During three months reaction, a small amount of silica containing species from the glass bottle walls was incorporated into the uranium rich phases.
v. Metallic iron surface was still available because of GR_C layer is porous and a big part (≈ 70%) of iron foil was light-reflecting *i.e.* not significantly corroded. However, a SEM micrograph for the whole cross section of iron foil shows that the thin uranium-rich layer and the UO_2 (s) crystals are only found on top of GR_C, but not on light-reflecting iron surface. This may be a possible explanation of the slightly faster initial U(VI) removal by the iron samples corroded for longer times, seen in Fig. 2.
vi. The thicker GR_C layer formed on the iron foil in the bottle B (1–5 μm), see Fig. 4a as compared to that on a iron grain in bottle A (0.5–1 μm) may be due to the presence of 10 ppm $UO_2(CO_3)_3^{4-}$ in bottle B which acts as an oxidant. This and the observation (v) above suggest that the GR_C can be formed from the redox reaction between U(VI) and Fe^0(or $Fe(OH)_2$).

Table 3. Result of EDS analysis for the points A–E marked in Fig. 4a, given in atomic %.

	A	B	C	D	E
O	26	56	61	44	76
Fe	54	37	37	55	4.5
U	8	3	0.5	0.2	17
Si	7	1	1	0.5	2
Cl	4	0.3	0.3	0.3	0.3

Most U(VI) in the synthetic groundwater was removed from the solution in a few days by metallic iron (see Fig. 2). This process may be followed by (a) the growth of layer-thickness and crystal size of GR_C and (b) the formation of UO_2 (s) crystals from U(IV) in the uranium-rich layer.

The stability of GR_C

The measured pH-E_h values and total Fe concentration for the solutions in the bottles C, D, E and F are listed in Table 4. At the experiment conditions, $C_{Fe(III)}$ is very low, therefore $C_{Fe(total)} \approx C_{Fe(II)}$. As shown in Fig. 3, all pH, E_h and $[Fe^{2+}]$ overlap in a small area marked by the black bar in the triangular field for GR_C. This shows that GR_C is stable under the experiment conditions in the present work.

In this work we have shown that, GR_C, as a major corrosion product of metallic iron at anoxic groundwater conditions, and with large surface area and positive surface charge, is more effective than metallic iron to remove U(VI) from anoxic synthetic groundwater.

The interactions between GR_C and transuranium elements and ^{99}Tc, as well as the stability of GR_C under strong radiation fields will be investigated in our laboratories.

Table 4. Measured pH, E_h and Fe concentration in batch reaction bottles C to F.

	bottle C cast iron 81 d	bottle D cast iron 44 d	bottle E pure iron 81 d	bottle F pure iron 44 d
pH	8.74	8.78	8.68	8.66
E_h, mV *vs*. SHE[a]	−515	−509	−402	−356
$C_{Fe\ total}$, 10^{-5} mol/L	1.7	1.9	0.84	0.53

a: $E_{h\ Ag/AgCl\ ref.+salt\ bridge} = 250\,mV + E_{h\ SHE}$.

Conclusions

Through this work, the following conclusions are drawn: (a) Under our simulated anoxic groundwater conditions, GR_C is the predominant corrosion product of metallic iron. (b) GR_C may also be produced from the redox reaction between U(VI) and Fe^0 or $Fe(OH)_2$). (c) GR_C on metallic iron is more efficient than the metallic iron to remove U(VI) from synthetic groundwater. (d) After three months ageing, most uranium was immobilised as UO_2 (s) crystals on top of GR_C.

Acknowledgment. The authors would like to thank Prof. Hansen H. C. (KVL, Denmark) for valuable discussion and comments, and Hans Bergqvist for SEM-EDS analysis. This work was supported by Swedish Nuclear Fuel and Waste Management Co. (SKB).

References

1. Gu, B., Liang, L. Dickey, J., Dai, S.: Reductive precipitation of uranium(VI) by zero-valent iron. J. Environ. Sci. Technol. **32**, 3366 (1998).
2. Eriksson, J., Werme, L.: Copper Canister with Cast inner Component. SKB TR 95-02 (1995).
3. Werme, L., Sellin, P., Kjellbert, N.: Copper Canisters for Nuclear High Level Waste Disposal. Corrosion Aspects, SKB TR 92-26 (1992).
4. KBS-3, Final Storage of Spend Nuclear Fuel. Report by the Swedish Nuclear Fuel Supply Co. Stockholm, Sweden (1983).
5. Loida, J., Grambow, B., Geckeis, H., Dressler, P.: Processes controlling radionuclide release from spent fuel. Mat. Res. Soc. Symp. Proc. **353**, 577 (1995).
6. Blackwood, D. J., Naish, C. C., Platts, N., Taylor, K. J., Thomas, M. I.: The Anaerobic Corrosion of Carbon Steel in Granitic Groundwater. SKB Project Report 95-03 (1995).
7. Stampfl, P. P.: Ein basisches Eisen-II-III Karbonat in Rost. Corrosion. Sci. **9**, 185 (1969).
8. Vatankhah, G., Drogowaska, M., Menard, H. J.: Electrodissolution of iron in sodium sulfate and sodium bicarbonate solution at pH 8. J. Appl. Electrochem. **28**, 173 (1998).
9. Drissi, S. H., Refait, P., Abdelmoula, M., Génin, J. M. R.: The preparation and thermodynamic properties of Fe(II)–Fe(III) hydroxide-carbonate (green rust I). Corr. Sci. **37**, 2025 (1995).
10. Génin, J. M., Bourrie, G, Trolard, F., Abdelmouta, M.: Thermodynamic equilibra in aqueous suspensions of synthetic and natural Fe(II)–Fe(II) Green Rust: occurrences of the mineral in hydromorphic soils. Environ. Sci. Technol. **32**, 1058 (1998).
11. Hansen, H. C. B.: Composition, stabilization and light absorption of Fe(II)Fe(III) hydroxy carbonate ('Green Rust'). Clay Mineral **24**, 663 (1989).
12. Bonin, P. M. L, Odziemkowski, M. S., Reardon, E. J., Gillham, R. W.: *In situ* identification of carbonate-containing Green Rust on iron electrodes in solutions simulating groundwater. J. Solution Chem. **29**, 1061 (2000).
13. Hansen, H. C. B.: Environmental Chemistry of Iron (II)-iron(III) LDHs (Green Rust). In: *Layered Double Hydroxides, Present and Future*. (Rives, V., ed.) Nova Science Publishers, Inc. (2001).
14. Loyaux-Lawniczak, S., Refrit, P., Erhardt, J.-J., Lecomte, P., Génin, J. M.-R.: Trapping of Cr by formation of ferrihydrite during the reduction of chromate ions by Fe(II)-Fe(III) hydroxysalt Green Rust. Environ. Sci. Technol. **34**, 435 (2000).
15. Williams, A. G. B, Scherer, M. M.: Kinetics of Chromate Reduction by Carbonate Green Rust. Preprint of Extended Abstracts, 220th ACS National Meeting, Washington DC 40 (2) (2000) pp. 666–668.
16. Levi, J. Izabel, C. Kaluzny, Y.: *Safety Assessment of Radioactive Repositories*. OECD, Paris (1990) p. 81.
17. Grenthe, I., Fuger, J., Konings, R. J. M., Lemire, R., Muller, A. B., Nguen-Trung, C., Wanner, H.: *Chemical Thermodynamics of Uranium.* Elsevier Science Publishers, Amsterdam (1992).
18. Fiedor, J. N., Bostick, W. D. Jarabek, R., Farrell, J.: Understanding the mechanism of uranium removal from groundwater by zero valent iron using X-ray photoelectron spectoscopy. Environ. Environ. Sci. Technol. **32**, 1466 (1998).
19. Farrel, J., Bostick, W. D., Jarabek, R., Fiedor, N.: Uranium removal from ground water using zero valent iron media. Ground Water **37**(4), 618 (1999).
20. Grambow, B., Smailos, E., Geckeis, H., Müller, R., Hentschel, H.: Sorption and reduction of uranium(VI) on iron corrosion products under reducing saline conditions. Radiochim. Acta **74**, 149 (1996).
21. Roh, Y., Lee, S. Y., Elless, M. P., Foss, J. E.: Incorporation of radioactive contaminants into pyroaurite-like phases by electrochemical synthesis. Clay Clay Minerals **48**, 266 (2000).
22. Cui, D., Eriksen, T.: Reduction of pertechnate by ferrous iron in solution, influence of sorbed and precipitated Fe(II). Environ. Sci. Technol. **30**, 2259 (1996).
23. Cui, D., Eriksen, T.: Reduction of pertechnate in solution by heterogeneous electron transfer from Fe(II) containing geological material. Environ. Sci. Technol. **30**, 2263 (1996).